The Fourth California Islands Symposium: Update on the Status of Resources
Edited by W. L. Halvorson and G. J. Maender. 1994. Santa Barbara Museum of Natural History, Santa Barbara, CA.

Petrology and Geochemistry of Miocene Volcanic Rocks from Santa Catalina and San Clemente Islands, California

Peter W. Weigand

Department of Geological Sciences, California State University,Northridge, CA 91330-8266
Tel. (818) 885-3541; Fax (818) 885-2820

Abstract. Major oxides and trace elements were analyzed in bulk-rock samples of middle Miocene volcanic rocks from Santa Catalina and San Clemente Islands located on the Southern California Continental Borderland. Volcanic rocks from Santa Catalina belong to the low- to medium-K calc-alkaline magma series and range in composition from basalt to rhyolite. Andesite samples have moderately fractionated rare-earth elements (La_N/Lu_N ~ 3.4) and have slight Eu anomalies (Eu/Eu^* ranges from 0.73 to 0.94). Two subsets of andesite samples have different degrees of REE enrichment; La_N averages 47 in 1 subset and 35 in the other. Spider-diagram patterns of the 2 sets are similar and exhibit only small fractionations.

Lavas on San Clemente belong to the medium-K calc-alkaline magma series and are compositionally bimodal: the dominant andesite unit has a range in SiO_2 content of 57 to 63 wt%, whereas the upper dacite and rhyolite units have a range of 69 to 70 wt% (rhyodacite). Andesite samples are moderately enriched in the light REE (La_N averages 59), are moderately fractionated (La_N/Lu_N = 3.7), and have small Eu anomalies (Eu/Eu^* = 0.74). Spider-diagram patterns show small depletions in Ta-Nb, Sr, P, and Ti.

Volcanic rocks from Santa Catalina and San Clemente Islands belong to a group of 12 volcanic centers that were active in southern California between 17 and 13 Ma. An average initial $^{87}Sr/^{86}Sr$ value of 0.7034 ± 0.0003 (n = 7) for samples of this group implies a mantle origin. Although this group of volcanic suites is calc-alkaline, a subduction-related origin cannot be reconciled with the history of plate motion in this area. During the middle Miocene, shear between the Pacific and North American plates began to be distributed across a wide belt, perhaps as the crust was heated by rising sub-continental mantle. Resulting localized extension in the mantle may have initiated decompression melting that produced widespread volcanism in coastal southern California.

Keywords: California; islands; Miocene; volcanic rocks; geochemistry.

Introduction

Igneous rocks of medial Miocene age crop out on about 17 named areas in coastal and offshore southern California, including 7 of the 8 southern California islands (Fig. 1), and are inferred to cover a significant portion of the California Borderland (e.g., Vedder et al. 1986). The cause of this widespread magmatism is unclear; theories fall into 4 general categories: (1) subduction of the Farallon plate beneath the North American plate, (2) southward migration of the Rivera triple junction, (3) overriding of the Pacific/Farallon spreading center, and (4) rifting of the lithospheric mantle as the Pacific and North American plates moved past each other. The timing of interaction between the Farallon, Pacific, and North American plates refined by Atwater (1989) effectively rules out the first 3 scenarios, and suggests that the Miocene igneous activity may have been the result of extension. In an early study of Neogene volcanic rocks in coastal southern California, Hawkins (1970) concluded that extensive volcanism originated in the mantle during regional dilation related to strike-slip faulting. Legg (1991) proposed that the extensive volcanism in the Southern California Continental Borderland was initiated by strike-slip related rifting (transtension) and that the volcanic flows on the 2 islands developed along the East Santa Cruz basin fault system that acted as a leaky transform fault. Both Santa Catalina and San Clemente Islands lie within what Crouch and Suppe (1993) term the "Los Angeles basin-inner borderland rift" and would represent rocks formed within the rift as the western Transverse Ranges block pivoted away from continental southern California. Weigand and Savage (1993) theorized that this rifting, whatever its origin, initiated decompression melting of the lithospheric mantle that resulted in the widespread Miocene volcanism.

This paper reviews previous work on volcanic rocks on Santa Catalina and San Clemente Islands, and new geochemical data are presented and discussed. It is shown below that these 2 volcanic centers share geochemical attributes with several other middle Miocene volcanic suites located south of Los Angeles in coastal and off-

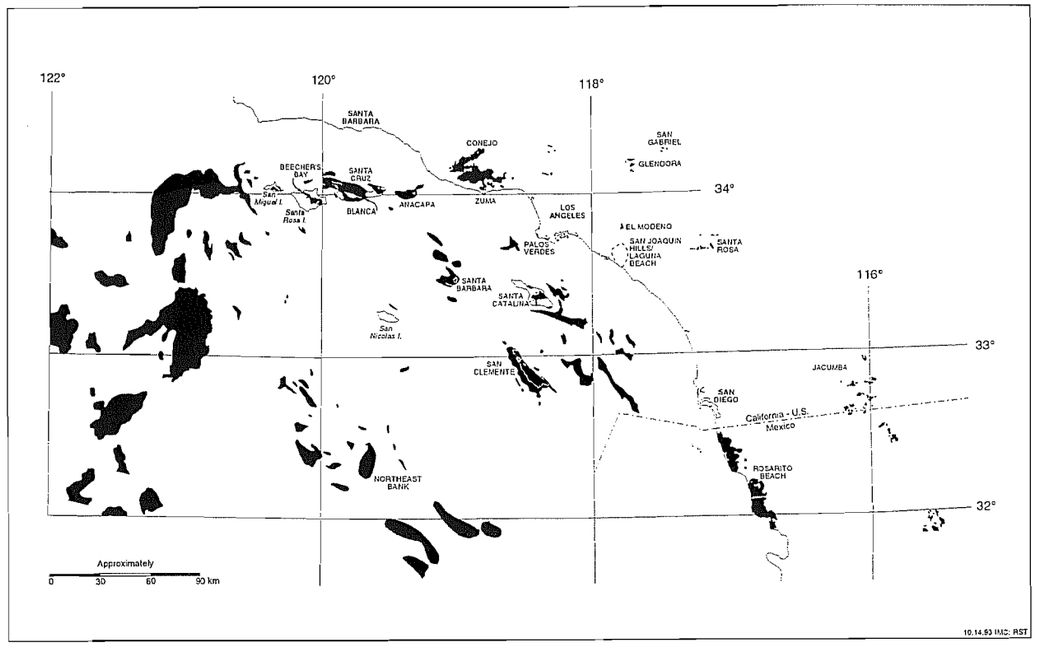

Figure 1. Map of Cenozoic volcanic areas in coastal and offshore southern California modified from Weigand and Savage (1993).

shore southern California and are collectively referred to as COSC (*Co*astal *s*outhern *C*alifornia) suites by Weigand and Savage (1993). The origin of these suites is then integrated into a tectono-magmatic model.

Santa Catalina Island

Santa Catalina Island is located on the inner borderland about 30 km southwest of the Palos Verdes Peninsula (Fig. 1). Miocene igneous activity on the island took 2 forms (Fig. 2). A hornblende quartz diorite pluton intruded into Catalina Schist basement 19.5 ± 0.6 Ma (Vedder et al. 1979). This pluton covers an area of about 39 km² on the island and also crops out offshore over an additional area of about 7 km². With the exception of a single whole-rock major-oxide analysis (Vedder et al. 1979), no geochemical work has been performed on this body.

Unconformably overlying the schistose basement and diorite pluton is a formerly extensive sequence of volcanic and sedimentary rocks now limited to 1 broad area midway between Avalon and the Isthmus and several other small areas. Volcanic rocks crop out over an area of about 32 km² on the island (Vedder et al. 1986). Surrounding much of the island is a unit of undifferentiated terrace deposits of late Miocene and Quaternary age; underlying this are additional exposures of Miocene volcanic rocks that cover about 190 km² (Vedder et al. 1986). Vedder et al. (1979) mapped in detail the volcanic and sedimentary sequence in the Fisherman's Cove, Cactus Peak-Cottonwood Canyon, and East End Quarry areas. The Fisherman's Cove sequence exceeds 150 m in thickness and is composed of a wide variety of fine-grained sedimentary rocks, volcanic and sedimentary breccias, extrusive flows and domes, and tabular intrusions. Vedder et al. (1979) determined that volcanism began about 14.7 Ma and extended until some time after 12.4 Ma, and ascribed the igneous and depositional activity and concomitant crustal deformation to the encroachment of the Pacific-Farallon ridge and the southward passage of the Rivera triple junction. Stewart et al. (1992) measured initial Nd isotopic ratios in samples from some of the major igneous units on Santa Catalina. A basaltic-andesite flow yielded an epsilon Nd value of +9.4 and more felsic samples yielded values of +4.1 to +6.1. They interpreted these data to imply that the mafic magmas originated from depleted mantle during ridge subduction associated with triple-junction migration.

Wood's (1981) study of the volcanic rocks of the Black Jack Peak-Whitley's Peak area included detailed field descriptions, modal analyses, microprobe analyses of phenocrysts, and chemical analyses. In this area, Wood found the volcanic section to be composed of subaerially deposited lava flows, laharic breccias, and tabular and dome intrusions that exceed 400 m in thickness. He estimated the following abundances of rock types: 5% basalt,

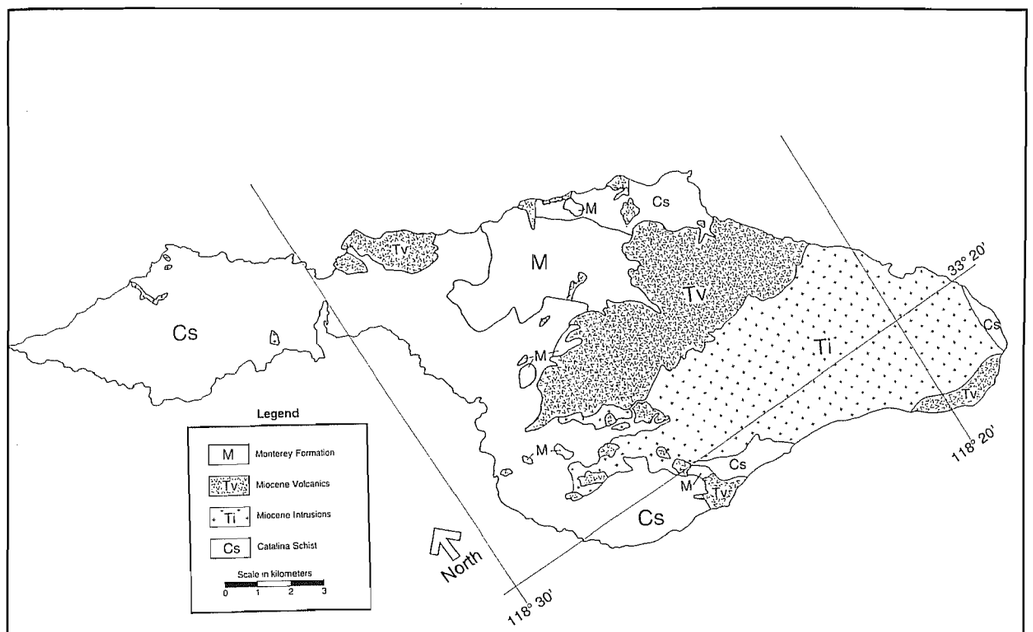

Figure 2. Generalized geologic map of Santa Catalina Island modified from Bailey (1985). Ti is hornblende quartz diorite and Tv is composed of a variety of volcanic and shallow intrusive units and sedimentary units.

Table 1. Microprobe analyses of phenocrysts from Santa Catalina volcanics (from Wood, 1981).

	Basalt	Basaltic andesite	Andesite	Dacite
Olivine	Fo_{79-77}	—	—	—
Plagioclase	An_{64-61}	An_{61-49}	An_{47-42}	An_{48-40}
Augite	Rare	$En_{48}Wo_{37}Fs_{16}$	$En_{43}Wo_{39}Fs_{18}$	Present
Hypersthene	—	$En_{72}Wo_{3}Fs_{25}$	$En_{70}Wo_{2}Fs_{28}$	Present
Hornblende	—	—	—	Present
Quartz	—	—	—	Present

17% basaltic-andesite, 35% andesite, 40% dacite, and 5% rhyolite. A summary of Wood's (1981) microprobe analyses of phenocrysts is given in Table 1. Chemical analyses show that the suite is low- to medium-K and calc-alkaline and that moderately high TiO_2 (> 1.0 wt%) and the absence of Fe-enrichment typify these rocks. Hurst (1983) reported initial $^{87}Sr/^{86}Sr$ values for 2 basalt samples, 0.70294 and 0.70344. Hurst et al. (1982) suggested

Table 2. Analyses of andesite samples from Santa Catalina Island.

	Ecb 1	TA 29	TA 22	R 3	TNAI	AVD	TA 12	TA 51	TPA5	TDX	C 4	C 2	BASS
SiO_2	55.70	56.00	56.80	56.60	56.50	57.30	57.80	58.10	59.50	61.70	61.80	61.80	62.70
TiO_2	1.27	1.25	1.24	1.34	1.25	0.90	0.90	0.88	0.93	0.57	1.21	1.27	0.86
Al_2O_3	18.00	17.20	17.20	16.80	17.50	16.80	17.00	16.80	17.00	16.70	18.00	16.90	16.40
FeO_T	6.85	6.07	6.24	6.36	6.06	5.20	5.34	5.24	5.04	4.06	5.23	5.52	4.56
MnO	0.13	0.12	0.15	0.17	0.11	0.12	0.15	0.14	0.10	0.09	0.07	0.10	0.08
MgO	4.45	3.94	4.21	4.13	4.19	4.87	4.32	4.30	4.12	1.38	1.95	2.10	3.22
CaO	8.06	7.36	7.33	7.53	8.59	7.57	6.89	6.93	6.22	4.13	5.36	4.65	5.88
Na_2O	3.48	3.65	3.57	3.46	3.67	3.55	3.58	3.86	3.55	3.89	4.42	4.57	3.99
K_2O	0.91	1.03	0.94	0.68	0.76	0.62	0.73	0.97	0.92	1.46	1.16	1.07	0.70
P_2O_5	0.18	0.23	0.22	0.21	0.18	0.14	0.17	0.18	0.18	0.21	0.22	0.21	0.17
H_2O	—	1.42	1.48	—	—	—	0.91	0.80	—	—	—	1.40	—
Total	99.03	98.27	99.38	97.28	98.81	97.07	97.79	98.20	97.56	94.19	99.42	99.59	98.56
Cr	162	50	55	58	116	142	137	134	121	9	15	15	102
Ni	65	49	61	70	57	60	58	54	72	42	0	59	102
Zn	94	79	80	80	87	72	80	73	73	69	76	75	66
Sc	25.7	19.2	19.1	19.1	21.3	18.6	18.3	17.4	16.7	7.6	14.1	14.4	14.0
Rb	31	35	41	12	17	20	26	31	35	35	32	48	18
Sr	312	241	337	245	307	349	418	353	411	318	456	300	296
Cs	1.9	7.7	5.5	7.0	2.3	0.6	0.7	1.0	1.0	1.5	58.7	34.9	6.7
Ba	358	568	619	537	614	334	373	316	337	581	831	626	458
Zr	165	158	124	146	136	127	133	102	102	97	178	133	104
Sb	BD	0.8	0.2	0.2	0.8	1.2	0.2	0.3	0.3	0.8	0.6	0.5	0.2
Hf	4.0	4.8	4.8	4.7	4.1	3.0	3.2	3.6	3.5	4.1	5.4	5.1	3.8
U	BD	BD	BD	1.2	BD	0.8	BD	BD	BD	0.9	2.2	1.9	1.6
Th	2.6	3.9	4.1	4.2	3.3	1.8	2.2	2.5	2.5	2.8	5.8	6.0	2.8
La	11.5	16.3	17.2	16.2	11.9	7.7	11.1	12.9	11.5	13.5	18.2	16.8	12.7
Ce	21.4	28.9	28.0	28.6	22.7	15.2	18.5	22.0	21.1	25.4	35.2	34.1	22.8
Nd	15.9	19.5	19.4	20.0	14.4	9.6	11.5	17.2	12.8	14.5	20.8	17.5	14.8
Sm	4.27	5.79	5.44	5.23	4.31	2.86	3.66	3.95	3.85	3.73	5.21	4.98	3.95
Eu	1.32	1.42	1.33	1.37	1.22	0.97	1.15	1.19	1.10	1.07	1.25	1.26	1.13
Tb	0.83	0.85	0.89	0.93	0.76	0.57	0.65	0.63	0.63	0.53	0.73	0.86	0.66
Yb	4.76	3.90	3.04	3.03	3.26	2.03	1.92	2.37	2.56	2.43	4.16	3.13	2.38
Lu	0.51	0.56	0.50	0.45	0.47	0.29	0.32	0.38	0.32	0.35	0.46	0.46	0.37

Major oxides in wt % (from Wood [1981]). FeO_T is total Fe expressed as FeO. Trace elements in parts per million (ppm).

that the Catalina magmas originated in a dilational environment generated as the Rivera triple junction interacted with the North American plate.

Table 2 lists geochemical analyses of selected andesite samples from Santa Catalina. The major oxides, analyzed by atomic absorption and spectrophotometric

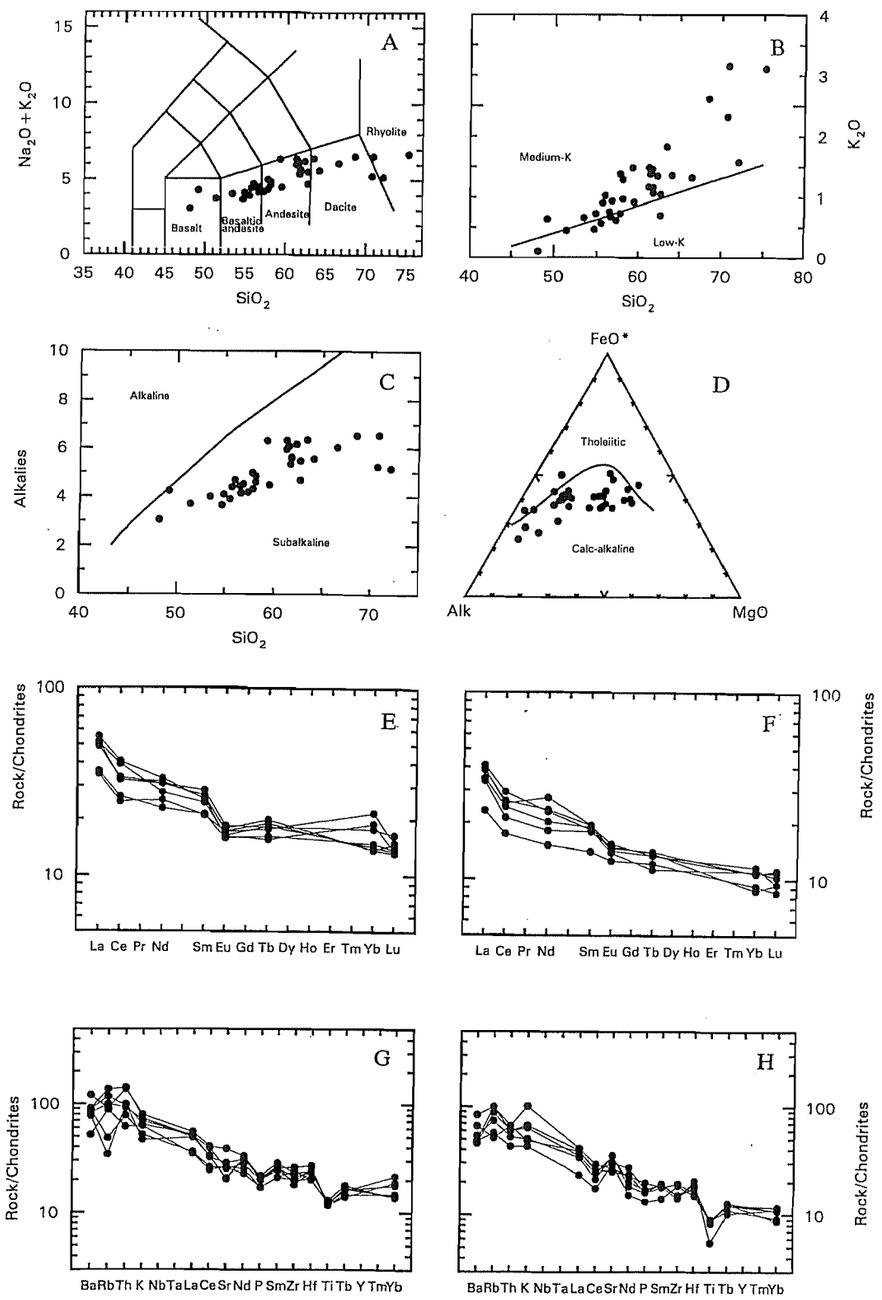

Figure 3. Geochemical diagrams for Santa Catalina samples. **3A.** Rock names of individual samples; boundaries from Le Bas et al. (1986). **3B.** K_2O series; boundaries from Gill (1981, p. 6). **3C** and **3D.** Alkalies-silica and AFM diagrams for magma series; boundaries from Irvine and Baragar (1971). Alk = Na_2O + K_2O. **3E.** Rare-earth element diagram for high Lu samples; normalizing data from Nakamura (1974). **3F.** Rare-earth element diagram for low Lu samples. **3G.** Spider diagram for high Lu samples; normalizing data from Thompson et al. (1984). **3H.** Spider diagram for low Lu samples.

methods, are from Wood (1981). The trace-element analyses are new and were performed by instrumental neutron activation methods. Figures 3a–d, which includes data from Vedder et al. (1979) and Wood (1981), confirms that the Santa Catalina volcanic rocks are calc-alkaline and low-K. The single available analysis of the 19.5-Ma hornblende quartz diorite (Vedder et al. 1979) is compositionally similar to andesite on Catalina with the exception of higher Na_2O and lower P_2O_5. This similarity strengthens the conclusion by Vedder et al. (1979) that the pluton and the younger lavas have a close genetic relationship.

Plots of the rare-earth elements (REE) normalized to chondritic meteorites (Fig. 3e-f) are characterized by slight enrichment of the light REE (La_N/Lu_N ~3.4) and slight negative Eu anomalies (Eu/Eu* ranges from 0.73 to 0.94, where Eu* is the concentration of Eu calculated by interpolating between its neighbors on the REE pattern). These plots reveal 2 subsets of samples, a lower SiO_2 group in which La_N averages 47 and a higher SiO_2 group in which La_N averages 35. Patterns on spider diagrams, also normalized to chondrites, of the 2 groups are similar and exhibit only small fractionations (Fig. 3g-h); most samples show a small negative spike for Ti and a few show a positive spike for Ce. The group of samples with higher La contents has slightly higher concentrations of all of these incompatible elements.

Although several analyzed Catalina samples are classified as basalt (Fig. 3a), none can be considered particularly primitive. The highest Ni abundance is 102 ppm, the highest Cr abundance is 162 ppm, and the highest Mg# is 65.

Crystal fractionation models were calculated using 3 representative samples that span the compositional range from basalt to rhyolite. A 2-stage model was used in which a representative basalt (SiO_2 = 50.0 wt%) was considered parental to a representative dacite (SiO_2 = 63.0 wt%), and then that dacite was considered parental to a representative rhyolite (SiO_2 = 71.0 wt%). Mineral analyses used were microprobe analyses of phenocrysts from Wood (1981). Results of the calculations (Table 3) yield low sums of squares of residuals (sosor) that indicate a good fit in both cases. The large amount of plagioclase suggested for both stages is consistent with its high abundance in rocks of mafic to intermediate composition. The presence of olivine and augite in the first stage corresponds to their presence in Catalina basalts; similarly, the presence of hornblende in the second stage corresponds to its common presence in Catalina dacites. These models, based on major oxides, were then tested using trace elements. Compositional trends of both compatible elements such as Ni and Cr and incompatible elements such as Rb and Zr can be successfully reproduced using the mineral assemblages of Table 3.

Table 3. Summary of modelling calculations for Santa Catalina samples.

Parent	basalt		dacite	
Daughter	dacite		rhyolite	
% Mineral subtracted				
Olivine	6.1		0	
Augite	22.2		0	
Plagioclase (% An)	43.1	(62)	33.4	(30)
Hornblende	0		9.4	
Magnetite	5.9		3.1	
% Liquid left	22.6		50.0	
SOSOR	0.14		0.04	

SOSOR = *S*um *O*f *S*quares *O*f *R*esiduals (see text).

San Clemente Island

San Clemente Island lies about 50 km WNW of San Diego (Fig. 1). It is the emerged portion of a structural block bounded on the northeast by the San Clemente fault that has a vertical displacement of at least 500 m (Junger 1976). Legg et al. (1989) considered this fault to be an active, right-lateral, strike-slip fault within the broad Pacific-North American transform plate boundary. The entire island consists of Miocene volcanic rocks that in places are interbedded with Miocene sedimentary rocks or blanketed by Quaternary sedimentary rocks and unconsolidated sediments (Fig. 4; Smith 1897; Olmsted 1958). Excluding the Quaternary cover, volcanic rocks crop out over an area of about 160 km² (Olmsted 1958). An additional 172 km² of volcanic rocks surround the island (Vedder et al. 1986). Unlike Santa Catalina, no older basement rocks crop out on San Clemente. Also, submarine volcanism predominated on San Clemente (Vedder and Howell 1976), whereas subaerial volcanic rocks are found on Santa Catalina.

Much of the following review of the volcanic rocks is summarized from Olmsted (1958). Andesite flows and minor pyroclastic units that exceed 600 m in thickness dominate the bulk of the island. Andesite varies from dense to highly vesicular with sparse to abundant phenocrysts. Phenocrysts are mostly plagioclase (~An_{50}) with less abundant augite and hypersthene. Groundmass textures vary from hyalopilitic to holocrystalline. Dacite occurs as 2 or more distinct flows that overlie the andesite and that reach 70 m in thickness. It is characterized by flow banding and is aphanitic to slightly porphyritic. Phenocrysts of mostly andesine plagioclase (An_{45-40}) and sparse hypersthene and augite are set in a pilotaxitic groundmass. Flows and minor tuff of rhyolite composition up to 45 m thick also overlie the andesite flows; rhyolite and dacite are not in contact with each other.

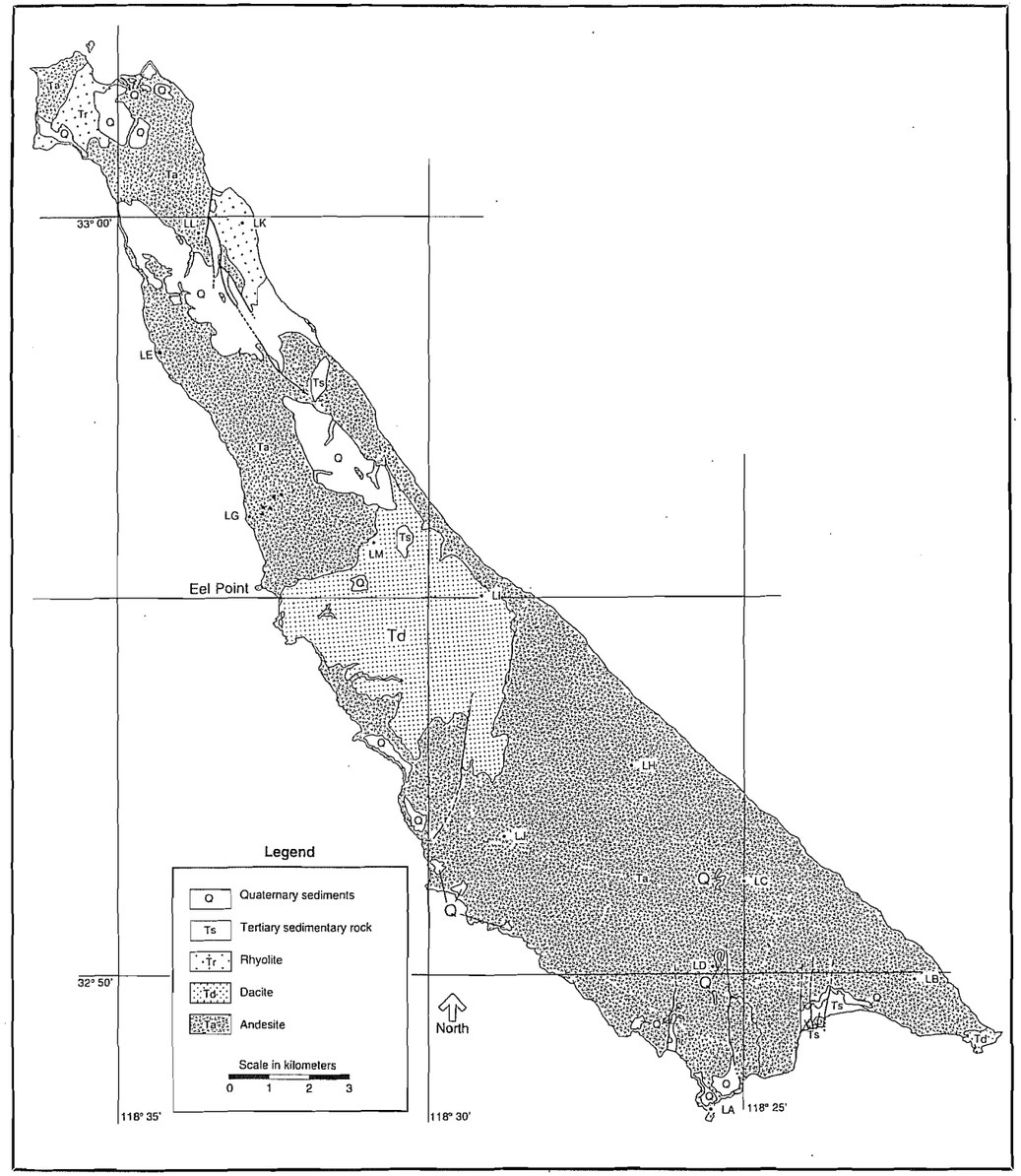

Figure 4. Generalized geologic map of San Clemente Island modified from Olmsted (1958).

Phenocrysts are predominantly andesine (An_{45-40}) and minor hypersthene, augite, and quartz.

Merifield et al. (1971) described the petrology of a core drilled at Eel Point, which is located about mid-island on the southwest coast (Fig. 4). About 364 m of andesite were encountered, which are largely not exposed on the island. The andesite is composed of phenocrysts of plagioclase (~35%), augite (~5%), and hypersthene (< 1%) set in a matrix containing variable amounts of feldspar, pyroxene, and glass. Phenocrystic plagioclase

Table 4. Major-oxide whole-rock analyses of samples from San Clemente Island.

Unit	Ta	Ta	Ta	Ta	Ta	Ta	Ta	Ta
Site	LA	LA	LB	LB	LC	LE	LGA	LGC
Sample	1	6	24	26	31	61	69	83
SiO_2	59.14	57.05	62.62	61.67	62.40	58.75	57.72	58.40
TiO_2	1.49	1.44	1.10	1.13	1.10	1.12	1.16	1.18
Al_2O_3	15.86	15.79	15.52	15.02	15.73	15.46	15.90	15.64
FeO_T	6.79	6.68	5.70	5.60	5.58	5.85	5.83	6.01
MnO	0.12	0.12	0.10	0.10	0.10	0.11	0.15	0.10
MgO	4.17	3.93	2.45	2.42	2.50	5.15	4.66	4.28
CaO	6.73	6.87	4.77	4.72	5.07	6.25	7.17	6.37
Na_2O	4.55	5.11	4.84	4.66	4.39	4.75	4.13	8.43
K_2O	1.28	1.21	1.83	1.87	1.96	1.49	1.26	1.26
P_2O_5	0.07	0.23	0.19	0.20	0.13	0.21	19.18	0.03
Total	100.20	98.43	99.12	97.39	98.96	98.06	99.12	101.70

Unit	Ta	Ta	Ta	Ta	Ta	Ta	Ta
Site	LGC	LGC	LGC	LGD	LGE	LGG	LGG
Sample	85	86	87	96	106	109	112
SiO_2	58.09	58.19	58.12	58.52	57.83	61.70	60.81
TiO_2	1.17	1.16	1.17	1.17	1.12	1.17	1.15
Al_2O_3	16.36	15.82	15.68	15.79	16.27	16.04	15.85
FeO_T	5.84	5.91	6.23	5.82	5.45	5.55	5.10
MnO	0.10	0.11	0.11	0.12	0.09	0.09	0.08
MgO	4.23	4.26	4.53	4.45	4.53	3.45	3.57
CaO	6.76	6.66	6.16	6.65	6.71	5.56	5.56
Na_2O	4.35	4.50	4.30	4.86	4.69	4.05	4.02
K_2O	1.24	1.24	1.24	1.34	1.35	1.83	1.86
P_2O_5	0.25	0.21	0.18	0.19	0.18	0.18	0.18
Total	98.39	98.06	97.72	98.91	98.22	99.62	98.18

Unit	Ta	Ta	Ta	Tr	Ta	Ta	Td
Site	LGH	LGH	LH	LK	LL	LL	LM
Sample	117	120	139	165	176	179	182
SiO_2	58.80	59.04	60.50	69.83	62.13	61.83	69.26
TiO_2	1.08	1.10	1.35	0.59	1.06	1.07	0.58
Al_2O_3	15.39	15.26	15.66	15.37	17.10	16.23	15.12
FeO_T	6.13	5.88	6.15	2.34	4.70	4.62	3.66
MnO	0.10	0.10	0.11	0.01	0.06	0.07	0.04
MgO	5.45	5.26	3.86	0.61	2.41	2.55	0.78
CaO	6.15	6.07	6.16	2.49	5.73	5.50	2.44
Na_2O	4.36	6.29	4.51	4.47	4.59	4.43	5.00
K_2O	1.23	1.30	1.46	2.49	1.86	1.90	2.48
P_2O_5	0.03	0.05	0.22	0.99	0.18	0.14	0.12
Total	98.72	100.35	99.98	99.19	99.82	98.34	99.48

Site refers to collecting sites on Figure 4. Major oxides in wt %. FeO_T is total Fe expressed as FeO.

ranges in composition from cores up to An_{78} to rims down to An_{47}. Hawkins and Hawkins (1977) reported phenocryst compositions of hypersthene ($W_4En_{67}Fs_{29}$) and augite ($Wo_{38}En_{45}Fs_{17}$) in San Clemente andesite and dacite.

Merifield et al. (1971) reported a whole-rock K-Ar date determined from near the bottom of the Eel Point core of 16.1 ± 0.8 Ma and one from near the top of the core of 15.9 ± 0.7 Ma. Turner (1970) reported additional K-Ar ages on plagioclase separates of 15.4 ± 1 Ma from a subaerial andesite flow and 13.6 ± 0.4 Ma from a rhyolite collected near the top of the volcanic sequence. Thus, volcanism lasted about 2.5 m. y. and probably longer if older volcanic rocks exist below the bottom of the core hole.

Hawkins and Divis (1975) reported initial $^{87}Sr/^{86}Sr$ values of 0.7042 on an andesite and 0.7045 on a rhyolite; Johnson and O'Neil (1984) reported an initial $^{87}Sr/^{86}Sr$ value of 0.70371 and a value for $\delta^{18}O$ of 6.8‰ on the rhyolite sample dated by Turner.

Tables 4 and 5 list whole-rock major-oxide analyses of samples from paleomagnetic drill cores (Luyendyk et al. 1988: sample numbers are keyed to sites shown on Fig. 4). These samples, largely andesite, are calc-alkaline and medium-K (Figs. 5a–d). Samples collected from Olmsted's (1958) lower andesite unit are all classified as andesite based on SiO_2 abundances, which range from 57.0 to 62.6 wt%. Collecting area LG represents 6 separate sites located near a dirt road that extends from near Black Point west to the coast (Fig. 4). Increasing sample numbers represent sites positioned higher in the section. Elevations range from 25 ft above sea level for site LGA to about 675 ft at site LGH. Samples from 5 of the sites are virtually indistinguishable (SiO_2 = 57.7 to 59.0 wt%) whereas the 2 samples from site LGG (475 ft elevation) have slightly higher SiO_2 abundances (60.8 to 61.7 wt%). The 2 samples from site LL, which is located in Olmsted's (1958) porphyritic andesite unit, exhibit no differences in major oxides compared to samples from the main andesite unit. The 3 samples collected from the dacite and rhyolite units are identical to each other with respect to major oxides.

Trace-element analyses of 4 representative andesite samples are listed in Table 5. Rare-earth patterns are straight (Fig. 5e) and exhibit slight light REE enrichment (La_N/Lu_N = 3.7) and small negative Eu anomalies (Eu/Eu* = 0.74). Concentrations of Gd may be somewhat elevated due to analytical difficulties (M. Walawender 1993, pers. comm.), which would exaggerate these negative Eu anomalies. Spider diagrams (Fig. 5f) exhibit negative spikes for Ti, P, Sr, and possibly Ba, and a small Ta-Nb trough.

None of the analyzed Clemente samples can be considered primitive. No basalt or basaltic-andesite have been reported from the island. The highest Ni abundance is 50 ppm, the highest Cr, 169 ppm, and the highest Mg# is 61.

Results of least-squares calculations of fractional crystallization models show that andesite sample SCL 66

Table 5. Major-oxide and trace-element whole-rock analyses of samples from San Clemente Island.

Unit	Ta	Ta	Ta	Td
Site	LC	LGA	LH	LI
Sample	33	66	137	148
SiO_2	63.40	58.50	61.10	69.90
TiO_2	1.10	1.20	1.39	0.54
Al_2O_3	15.30	15.20	14.80	14.50
FeO_T	5.16	5.56	5.62	3.05
MnO	0.08	0.09	0.10	0.03
MgO	2.24	4.46	3.51	0.48
CaO	4.87	6.64	5.68	2.11
Na_2O	4.36	3.89	4.32	5.22
K_2O	1.58	1.33	1.19	2.24
P_2O_5	0.24	0.18	0.23	0.10
LOI	1.16	1.39	0.93	1.23
Total	99.49	98.44	98.87	99.40
V	120	150	170	34
Cr	34	169	85	11
Ni	12	50	43	7
Co	13	24	22	5.2
Cu	22	39	35	11
Zn	89	87	93	57
Sc	15.9	21.6	20.3	8.39
Rb	69	56	56	106
Sr	250	250	260	190
Cs	3.0	1.3	2.1	1.10
Ba	510	320	360	600
Y	75	47	45	37
Zr	250	190	210	330
Nb	14	12	11	16
Sb	0.2	0.2	0.3	0.3
Hf	6.7	4.5	5.4	8.2
Ta	0.5	0.5	0.7	0.7
U	1.5	1.5	1.4	2.1
Th	4.4	3.8	3.7	6.1
La	24.5	18.7	15.3	19.2
Ce	42	42	35	41
Nd	26	23	19	20
Sm	6.15	5.64	4.71	4.59
Eu	1.80	1.49	1.68	1.14
Gd	10.1	8.3	6.4	6.1
Tb	1.3	1.2	0.8	0.9
Dy	8.9	7.8	6.5	5.7
Yb	4.58	3.53	3.02	3.18

Major oxides in wt %. FeO_T is total Fe expressed as FeO. LOI = Loss On Ignition. Trace elements in parts per million (ppm). Analytical methods listed in Weigand and Savage (1993).

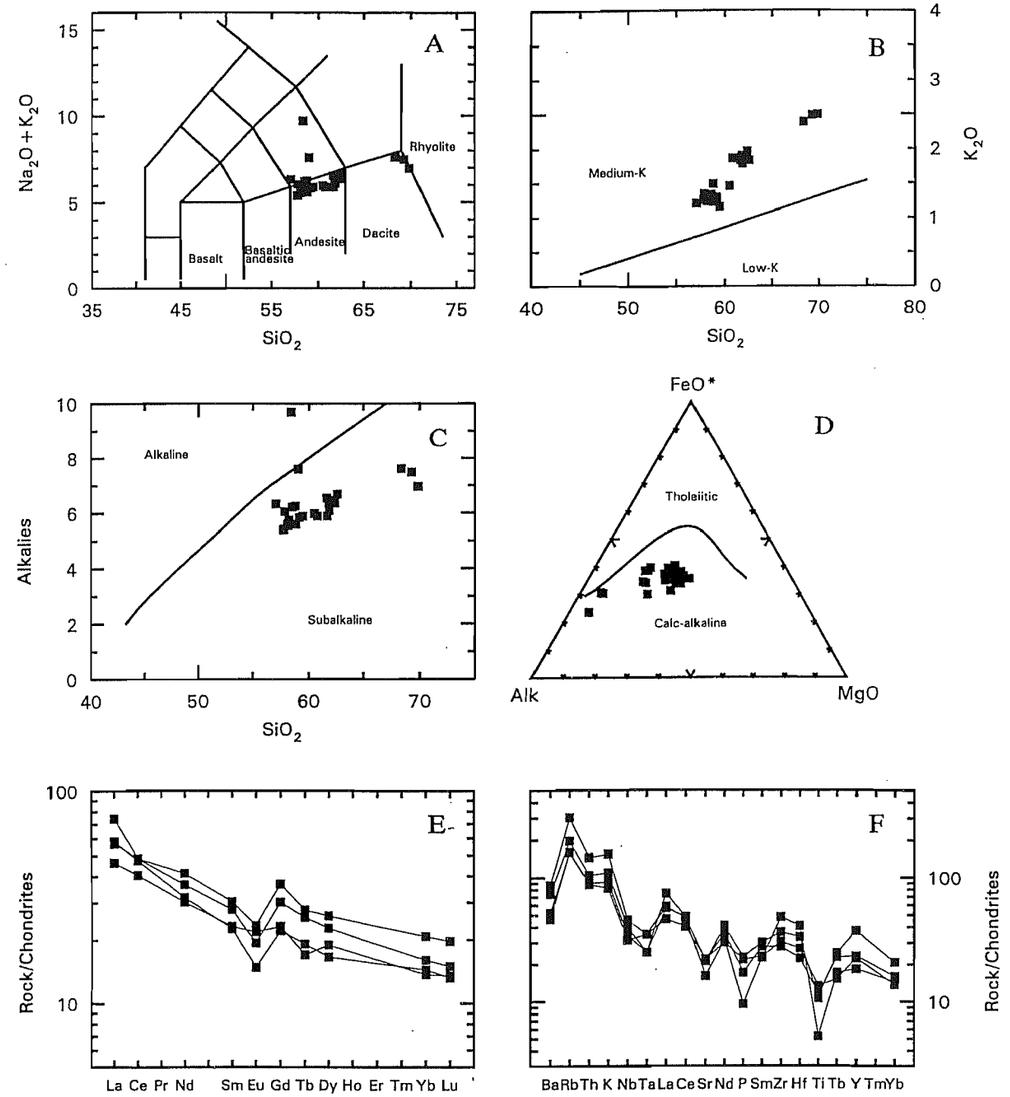

Figure 5. Geochemical diagrams for San Clemente samples. **5A.** Rock names of individual samples. **5B.** K_2O series. **5C.** Alkalies-silica diagram. **5D.** AFM diagram. **5E.** Rare-earth element diagram. **5F.** Spider diagram.

(SiO_2 = 58.50 wt%) can yield dacite sample SCL 33 (SiO_2 = 63.40 wt%) by the subtraction of an assemblage of plagioclase (An_{50}), augite ($Wo_{41}En_{50}Fs_{10}$), hypersthene ($Wo_4En_{80}Fs_{15}$), and magnetite (Table 6). The same parent can yield dacite sample SCL 148 (SiO_2 = 69.90 wt%) by the subtraction of different proportions of the same minerals. The validity of these calculations is strengthened by the fact that these are the same minerals found as phenocrysts in San Clemente andesite and the proportions are in the same order (Merifield et al. 1971). In addition, subtraction of these assemblages reproduces the variations exhibited by a variety of trace elements.

Table 6. Summary of modelling calculations for San Clemente samples.

Parent	andesite LGA 66	andesite LGA 66
Daughter	dacite LC 33	dacite LI 148
% Mineral subtracted		
Olivine	0	0
Augite	7.9	13.5
Hypersthene	5.8	7.5
Plagioclase	14.0	25.0
Magnetite	1.3	2.8
Ilmenite	0	0.9
% Liquid left	70.6	50.1
SOSOR	0.08	0.04

SOSOR = *S*um *O*f *S*quares *O*f *R*esiduals (see text).

Comparison

Volcanic rocks from Santa Catalina and San Clemente Islands belong to a group of 12 volcanic centers that were active in southern California between 17 and 13 Ma. The analyzed samples from these COSC suites show a preponderance of andesite, are calc-alkaline and have medium or medium-to-low contents of K. Two representative SiO_2-variation diagrams (Fig. 6) emphasize this relative homogeneity (data sources listed in Weigand 1994). Nevertheless, each area exhibits subtle differences. For instance, the Santa Catalina samples extend over a greater SiO_2 range than the other areas and have somewhat lower concentrations of TiO_2 and K_2O than those from the other areas. San Clemente samples have a somewhat higher concentration of MgO than those from the other areas. Samples from El Modeno are characterized by a very restricted range in SiO_2, whereas the Rosarito Beach and San Clemente suites exhibit a gap in SiO_2 contents. Some of the Rosarito samples also have the highest TiO_2 contents.

There are too few data to make many observations about trace elements. Rare-earth patterns show a modest enrichment of the light REE compared to chondrites (La_N ranges from 30 to 54) and compared to the heavy REE (La_N/Lu_N ranges from 3.1 to 5.3). Slight negative Eu-anomalies are shown by samples from only 2 areas; Eu/Eu* averages 0.85 for Santa Catalina andesites and 0.74 for San Clemente samples. San Clemente samples, the only ones for which reliable Ta and/or Nb data are available, exhibit a small negative Ta-Nb trough on the spider diagram.

Discussion

All of the COSC suites belong to the calc-alkaline magma series. Although only a few samples have a reliable data for Nb and/or Ta, those from San Clemente exhibit small but distinct Nb-Ta troughs on a spider diagram, which is a characteristic of subduction-related igneous rocks (Thompson et al. 1984). The success of the fractional crystallization modelling for the Santa Cruz and Santa Catalina suites, including the ability to reproduce trace-element patterns, suggests that fractionation of a low-temperature mineral assemblage was responsible for much, if not most, of the chemical variation exhibited for these rocks. Most of the rocks in COSC suites have undergone moderate degrees of fractionation, and no COSC samples have an Mg# > 65, Ni > 110 ppm, or Cr > 260 ppm, all far lower than values thought to be repre-

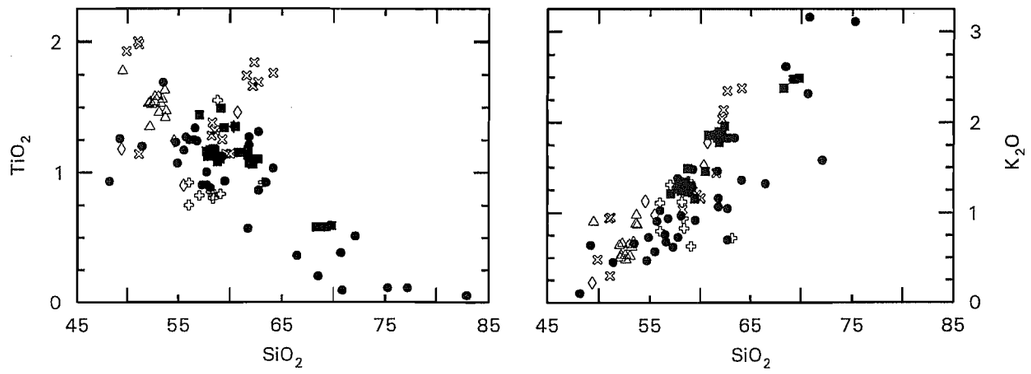

Figure 6. Comparison of Santa Catalina and San Clemente volcanic samples with other COSC suites. ● = Catalina; ■ = Clemente; △ = El Modeno; x = Rosarito Beach; ◇ = Palos Verdes; **cross** = Laguna Beach.

sentative of unmodified mantle melts [67, 400 to 500 ppm, and 1,000 ppm, respectively (Wilson 1989)].

Low values of both $^{87}Sr/^{86}Sr$ and $\delta^{18}O$, as well as relatively high values of epsilon Nd, in samples from these suites argue for derivation from a mantle source with little or no contribution from, or interaction with, continental crust—even for the more evolved dacite and rhyolite samples. Both the calc-alkaline nature of the volcanic rocks and the presence of a Nb-Ta depletion strongly suggest that these rocks were generated in a subduction setting. However, as outlined below, evidence from ocean-floor magnetic anomalies indicates that subduction in this area had ceased for some 3 to 10 my before volcanism began. Thus these rocks may represent calc-alkaline volcanic rocks that originated somewhere other than in a subduction environment.

The tectonic environment of magma generation responsible for the widespread volcanism in coastal and offshore southern California during the middle Miocene has generated much speculation. From sea-floor magnetic anomalies, Atwater (1989) has shown that subduction had ceased in this area 3–10 million yr before the main pulse of middle Miocene volcanism. Some authors have used paleomagnetic inclination data to suggest that the Baja-Borderland allochthon of southern California was transported from the south (e.g. Champion et al. 1986), raising the possibility that volcanism occurred in a subduction setting south of the Rivera triple junction before the Baja-Borderland allochthon was translated northward. However, sea-floor magnetic anomalies (Atwater 1989) and other evidence (Butler et al. 1991; Crouch and Suppe 1993) argue against such large-scale movements. Thus, plate configurations during the middle Miocene appear to preclude this widespread volcanic event from being related to subduction or triple-junction processes.

The tectonic environment in southern California at the time of Miocene volcanism was dominated by shear related to the dextral transform between the Pacific and North American plates. This shear affected a broad zone of continental crust that was possibly heated and softened by hot, mantle material that rose into a no-slab region created between the Mendocino and Rivera triple junctions (Henyey 1976). Across a wide area, basins were forming (Crowell 1974), large crustal blocks were rotating (Kamerling and Luyendyk 1979), and crust was rifting (Yeats 1968; Legg 1991; Crouch and Suppe 1993). This extensional environment provided an opportunity for decompression melting to develop in the lithospheric mantle, especially beneath the most highly extended areas such as the inner borderland.

Because igneous rocks belonging to the calc-alkaline magma series are currently erupting exclusively in subduction environments, prehistoric calc-alkaline suites are conventionally thought to require a subduction setting. However, Robyn (1975) interpreted some Miocene calc-alkaline volcanic rocks in eastern Oregon to have originated in an extensional rather than a subduction environment. Also, other recent studies have documented the presence of lavas with arc characteristics in non-arc settings (i.e., Lange et al. 1993; Sloman 1989). These studies suggest that the overlying mantle can stabilize fluids derived from the downgoing slab, and can subsequently yield arc-characterized magmas generated by tectonic events that postdate active subduction.

Lavas on San Clemente and Santa Catalina Islands specifically, and all related Miocene suites in coastal southern California in general, are concluded to have been generated by decompression melting beneath the Southern California Continental Borderland that was initiated by widespread extension. The lithospheric mantle source had attained its geochemical characteristics during subduction of the Farallon plate between about 220 Ma and 30 Ma. Later extension, associated with Pacific/North American shear, triggered short-lived but widespread volcanism in coastal and offshore southern California.

Acknowledgements. B. P. Luyendyk generously donated paleomagnetic core samples from San Clemente Island and W. R. Wood kindly donated samples from his thesis research. D. Jenson is thanked for his work on the San Clemente samples. The trace-element analyses were funded by the School of Science and Mathematics, CSUN, and by Oregon State University under a U.S. Department of Energy Reactor Use-Sharing Grant. D. Liggett, M. Walawender, J. Crouch, and M. Legg provided helpful editorial suggestions.

Literature cited

Atwater, T. 1989. Plate tectonic history of the northeast Pacific and western North America. In: The Eastern Pacific Ocean and Hawaii (edited by E. L. Winterer, D. M. Hussong, and R. W. Decker), Geological Society of America, The Geology of North America, N:21–72.

Bailey, E. H. 1985. Generalized geologic map of Santa Catalina Island, California. In: Geology of Santa Catalina Island (edited by E. L. Gath and M. M. Bottoms), South Coast Geological Society, Annual Field Trip Guidebook 13, p. 82.

Butler R. F., W. R. Dickinson, and G. E. Gehrels. 1991. Paleomagnetism of coastal California and Baja California: alternatives to large-scale northward transport. Tectonics 10:561–576.

Champion, D. E., D. G. Howell, and M. M. Marshall. 1986. Paleomagnetism of Cretaceous and Eocene strata, San Miguel Island, California Borderland and the northward translation of Baja California. Journal of Geophysical Research 91:11557–11570.

Crouch, J. K., and J. Suppe. 1993. Neogene tectonic evolution of the Los Angeles basin and inner borderland: a model for core complex-like crustal extension. Geological Society of America Bulletin 105:1415–1434.

Crowell, J. C. 1974. Origin of late Cenozoic basins in southern California. Society of Economic Paleontologists and Mineralogists Special Publication 22, pp. 190–204.

Gill, J. B. 1981. Orogenic andesites and plate tectonics. Springer-Verlag, Berlin. 389 pp.

Hawkins, J. W. 1970. Petrology and possible tectonic significance of late Cenozoic volcanic rocks, southern California and Baja California. Geological Society of America Bulletin 81:3323–3338.

Hawkins, J. W., and A. F. Divis. 1975. Petrology and geochemistry of mid-Miocene volcanism on San Clemente and Santa Catalina Islands and adjacent areas of the Southern California Borderland. Geological Society of America Abstracts with Programs 2:323–324.

Hawkins, J. W., and D. L. Hawkins. 1977. Petrology, geochemistry and evolution of mid-Miocene volcanic rocks of San Clemente Island, Southern California Borderland. Geological Society of America Abstracts with Programs 9:432.

Henyey, T. L. 1976. Heat flow and tectonic patterns on the southern California borderland. In: Aspects of the Geologic History of the California Continental Borderland (edited by D. G. Howell), Pacific Section, American Association of Petroleum Geologists Miscellaneous Publication 24, pp. 427–448.

Hurst, R. W. 1983. Volcanogenesis contemporaneous with mid-ocean ridge subduction and translation. In: The Significance of Trace Elements in Solving Petrogenetic Problems and Controversies, Theophrastus Publications S. A., Athens, Greece, pp. 197–213.

Hurst, R. W., W. R. Wood, and M. Hume. 1982. The petrologic and tectonic evolution of volcanic rocks in the southern California Borderland: a transitional tectonic environment. In: Mesozoic-Cenozoic Tectonic Evolution of the Colorado River Region, California, Arizona and Nevada (edited by E. Frost and D. Martin), Anderson-Hamilton Volume, Cordilleran Publication, San Diego, pp. 287–297.

Irvine, T. N., and W. R. A. Baragar. 1971. A guide to the chemical classification of the common volcanic rocks. Canadian Journal of Earth Science. 8:523–548.

Johnson, C. M., and J. R. O'Neil. 1984. Triple junction magmatism: a geochemical study of Neogene volcanic rocks in western California. Earth and Planetary Science Letters 71:241–262.

Junger, A. 1976. Tectonics of the Southern California Borderland. In: Aspects of the Geologic History of the California Continental Borderland (edited by D. G. Howell), Pacific Section, American Association of Petroleum Geologists Miscellaneous Publication 24, pp. 486–498.

Kamerling, M. J., and B. P. Luyendyk. 1979. Tectonic rotations of the Santa Monica Mountains region, western Transverse Ranges, California, suggested by paleomagnetic vectors. Geological Society of America Bulletin 90:331–337.

Lange, R. A., I. S. E. Charmichael, and P. R. Renne. 1993. Potassic volcanism near Mono basin, California: evidence for high water and oxygen fugacities inherited from subduction. Geology 21:949–952.

Le Bas, M. J., R. W. Le Maitre, A. Streckeisen, and B. Zanettin. 1986. A chemical classification of volcanic rocks based on the total alkali-silica diagram. Journal of Petrology 27:745–750.

Legg, M. R. 1991. Developments in understanding the tectonic evolution of the California Continental Borderland. In: From Shoreline to Abyss: Contributions in Marine Geology in Honor of Francis Parker Shepard (edited by R. Osborne), Society for Sedimentary Geology Special Publication 46, pp.290–312.

Legg, M. R., B. P. Luyendyk, J. Mammericxx, C. De Moustier, and R. C. Tyce. 1989. SeaBeam survey of an active strike-slip fault—The San Clemente fault in the California Continental Borderland. Journal of Geophysical Research 94:1727–1744.

Luyendyk, B. P., M. J. Kamerling, J. S. Hornafius, R. Haston, and J. N. Carter. 1988. Paleomagnetic studies in Neogene rocks from the Peninsular Ranges, southern California. Geological Society of America Abstracts with Programs 20:63.

Merifield, P. M., D. L. Lamar, and M. L. Stout. 1971. Geology of central San Clemente Island, California. Geological Society of America Bulletin 82:1989–1994.

Nakamura, N. 1974. Determination of REE, Ba, Fe, Mg, Na and K in carbonaceous and ordinary chondrites. Geochimica et Cosmochimica Acta 38:757–775.

Olmsted, F. H. 1958. Geologic reconnaissance of San Clemente Island, California. U.S. Geological Survey Bulletin 1071-B, pp. 55–68.

Robyn, T. L. 1979. Miocene volcanism in eastern Oregon: an example of calc-alkaline volcanism unrelated to subduction. Journal of Volcanology and Geothermal Research 5:149–161.

Sloman, L. E. 1989. Triassic shoshonites from the Dolomites, northern Italy: alkaline arc rocks in a strike-slip setting. Journal of Geophysical Research 94:4655–4666.

Smith, W. S. T. 1897. The geology of Santa Catalina Island. California Academy of Science Proceedings, 3rd Series, v. 1, 71 pp.

Stewart, B. W., G. E. Bebout, and M. Grove. 1992. Miocene magmatism in a transcurrent tectonic setting: isotopic data from Santa Catalina Island, California. Eos Transactions of the American Geophysical Union 73:338.

Thompson, R. N., M. A. Morrison, G. L. Hendry, and S. J. Parry. 1984. An assessment of the relative roles of a crust and mantle in magma genesis: an elemental approach. Philosophical Transactions of the Royal Society of London A310:549–590.

Turner, D. L. 1970. Potassium-argon dating of Pacific Coast Foraminiferal Stages. Geological Society of America Special Paper 124:91–129.

Vedder, J. G., and D. G. Howell. 1976. Neogene strata of the southern group of Channel Islands, California. In: Aspects of the Geologic History of the California Continental Borderland (edited by D. G. Howell), Pacific Section, American Association of Petroleum Geologists Miscellaneous Publication 24, pp. 80–106.

Vedder, J. G., D. G. Howell, and J. A. Forman. 1979. Miocene strata and their relation to other rocks, Santa Catalina Island, California. In: Cenozoic Paleogeography of the Western United States (edited by J. M. Armentrout, M. R. Cole, and H. TerBest, Jr.), Pacific Section, Society of Economic Paleontologists and Mineralogists, Pacific Coast Paleogeography Symposium 3:239–256.

Vedder, J. G., H. G. Greene, S. H. Clarke, and M. P. Kennedy. 1986. Geologic map of the mid-southern California continental margin. In: Geologic Map Series of the California Continental Margin (edited by H. G. Greene and M. Pp. Kennedy), California Division of Mines and Geology, Plate 2A, scale 1:250,000.

Weigand, P. W. 1994. Middle Miocene igneous rocks in the El Modeno, San Joaquin Hills, and Laguna Beach areas, southern California. In: Field Geology in Orange County, Southern California (edited by P. Hughes, R. P. Lozinsky, and G. R. Roquemore), Far Western Section National Association of Geology Teachers Guidebook, pp. 55–84.

Weigand, P. W., and K. L. Savage. 1993. Review of the Miocene volcanic rocks of the western Santa Monica Mountains, California. In: Miocene Sedimentary and Volcanic Environments, Santa Monica Mountains, California (edited by P. W. Weigand, A. E. Fritsche, and G. E. Davis), Society for Sedimentary Geology, Pacific Section, Book 72, pp. 93–112.

Wilson, M. 1989. Igneous Petrogenesis. Unwin and Hyman, London, 466 pp.

Wood, W. R. 1981. Geology, petrography and geochemistry of the Santa Catalina Island volcanic rocks, Black Jack Peak to Whitley's Peak area [M. S. Thesis]. California State University, Los Angeles, 146 pp.

Yeats, R. S. 1968. Rifting and rafting in the southern California borderland. In: Conference on Geologic Problems of the San Andreas Fault System (edited by W. R. Dickinson and A. Grantz), Stanford University Publications in Geological Sciences 11:307–322.

The Fourth California Islands Symposium: Update on the Status of Resources
Edited by W. L. Halvorson and G. J. Maender. 1994. Santa Barbara Museum of Natural History, Santa Barbara, CA.

Faulting and Uplift of the Northern Channel Islands, California

Christopher C. Sorlien

Institute for Crustal Studies, University of California, Santa Barbara, CA 93106
Tel. (805) 893-8231; Fax (805) 893-8649

Abstract. The northern Channel Islands are aligned E–W along the southern margin of the rotated western Transverse Ranges. Continuing post-Miocene clockwise rotation of the western Transverse Ranges is related to oblique left-reverse deformation of the northern Channel Islands. Strain partitioning is indicated by the presence of sub-horizontal striations on fault surfaces of both outcrop-scale and island-scale faults. Uplifted wavecut platforms are present in the footwalls (downthrown blocks) of the steeply-dipping mapped faults, and must be the result of thrust motion above sub-horizontal faults. On eastern Santa Cruz Island, as the upper crust moves southward relative to the deeper crust, new oblique-slip faults are progressively forming to the north.

The time that the islands have been emergent can be calculated from the elevation of the islands, the rock uplift rate, and the erosion rate. Because the wavecut rock platforms have yet to be dated, the uplift rate is not known. Well preserved wavecut platforms in volcanic rocks suggest that denudation of the highest peaks has been slow, and that uplift must have been at least a kilometer since important shortening initiated at the end of early Pliocene time. Large permanent islands have only been present for ~3 My, or ~2 My if shortening and uplift rates have increased with time.

Keywords: California; western Transverse Ranges; northern Channel Islands; rotation; uplift; faulting; striations; marine terraces; strain partitioning.

Introduction

The northern Channel Islands lie along the southern margin of the western Transverse Ranges, south of Santa Barbara Channel (Fig. 1). The Transverse Ranges are

Compiled from: Greene and Kennedy (1989); Jennings and Strand (1969); PG&E (1988); Junger and Wagner (1977); This Study

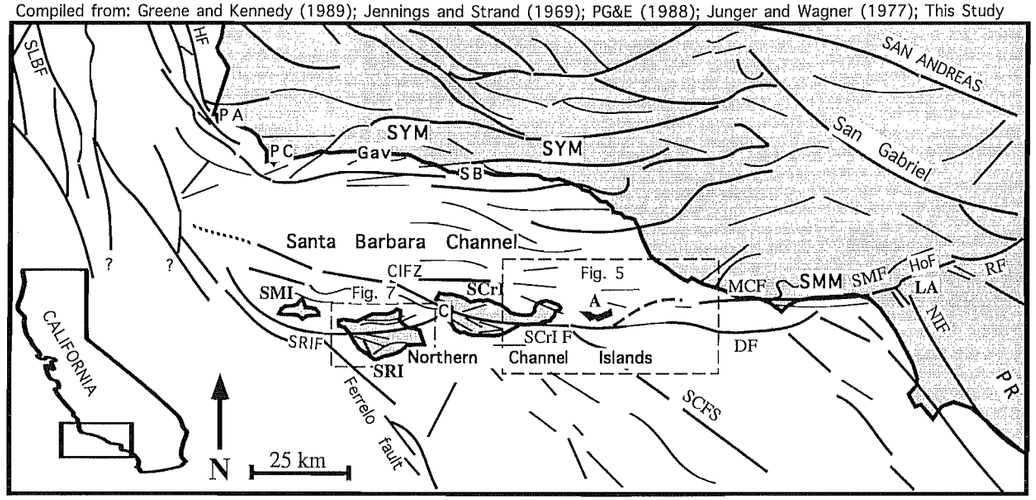

Figure 1. Faults and locations of the western Transverse Ranges. Geographic abbreviations include: **A** = Anacapa Island; **C** = Christi outcrop; **Gav** = Gaviota; **LA** = Los Angeles; **PA** = Point Arguello; **PC** = Point Conception; **PR** = Peninsular Ranges; **SB** = Santa Barbara; **SCrI** = Santa Cruz Island; **SMM** = Santa Monica Mountains; **SMI** = San Miguel Island; **SRI** = Santa Rosa Island; **SYM** = Santa Ynez Mountains; the western Transverse Ranges are the region of E-W faulting. Structural abbreviations include: **CIFZ** = Channel Islands fault zone of Ogle (1984); **DF** = Dume fault; **HF** = Hosgri fault; **HoF** = Hollywood fault; **MCF** = Malibu Coast fault; **NIF** = Newport-Inglewood fault; **RF** = Raymond fault; **SCFS** = San Clemente fault system (along the eastern escarpment of Santa Cruz-Catalina ridge); **SCrIF** = Santa Cruz Island fault; **SMF** = Santa Monica fault; **SRIF** = Santa Rosa Island fault; **SLBF** = Santa Lucia Bank fault.